Clays and Clay Minerals, Vol. 40, No. 1, 53–64, 1992.

SMECTITE-TO-ILLITE CONVERSION IN A GEOTHERMALLY AND LITHOLOGICALLY COMPLEX PERMIAN SEDIMENTARY SEQUENCE

C. BÜHMANN

Soil and Irrigation Research Institute, Private Bag X79
Pretoria 0001, Republic of South Africa

Abstract—The <0.5-μm fraction of 120 samples from a lithologically complex Permian sedimentary sequence, underlying dolerite intrusive sheets, has been characterized by means of X-ray diffraction to establish I/S compositions as a function of temperature, lithology and time duration. Illitization has been active over the entire 210 m depth range and the clay data reflect both the local pattern of contact metamorphism and the more regional trend of heat flow during burial. A continuum exists in the illite proportions of the illite/smectite interstratifications with increasing distance from the intrusive sheet ranging from R = 3 with less than 5% smectite via R = 2 and R = 1 to R = 0 with up to 70% smectite. In the mixed-lithology section, individual component layers in the I/S within similar distance levels, but between contrasting lithologies, appear to vary only within a very restricted compositional range. In the massive mudstone strata, however, more silty parts contain I/S of a higher degree of ordering and lower expandability. Calcite contents are reflected in a higher rate of chlorite formation, but not in the I/S composition. A satisfactory inverse correlation was found between percent smectite in I/S and vitrinite reflectance in the lithologically complex section. R = 1 interstratifications are associated with a maximum vitrinite reflectance of 1.07–1.29 and R > 1 phases with 1.93–2.7, indicating that time duration is not a controlling factor in the illitization process in this facies. R = 0 interstratifications are present in a massive mudstone/siltstone sequence situated furthest from the igneous intrusives, and display vitrinite reflectance values of 1.42–1.52. No satisfactory explanations for this finding can be offered.

Key Words— Burial diagenesis, Contact metamorphism, Lithology, Paleotemperature, Vitrinite reflectance.

INTRODUCTION

The conversion of smectite to illite is a major clay mineral reaction that occurs in a range of low-temperature geologic environments and is governed by several chemical and physical parameters (Ramseyer and Boles, 1986; Whitney, 1990). Temperature is considered the most important control (Hower *et al.*, 1976), and compositional trends in illite/smectite interstratifications (henceforth referred to as I/S) have been used as a geothermometer in several sedimentary basins (Heroux *et al.*, 1979; Hoffman and Hower, 1979; McDowell and Elders, 1980; Inoue and Utada, 1983; among many others). Calculated thermal gradients were constructed by Hoffman and Hower (1979) using isograds based on temperatures of the disappearance of smectite (70°C), the occurrence of R = 1 I/S (100°C), and the first occurrence of R = 3 I/S (180°C).

While reports on I/S compositions in burial environments are common, information on clay mineralogical trends in the vicinity of intrusive bodies are scarce (Nadeau and Reynolds, 1981; Smart and Clayton, 1985; Aaron and Lee, 1986). The major difference between burial diagenetic and contact metamorphic processes is the time duration and contrasting information is available as to its influence on the illitization reaction. According to Smart and Clayton (1985), for example, the progressive illitization of I/S occurs too slowly to reflect the thermal effects of a minor, 50 m-thick igneous intrusive, except close to the contact. Środoń (1979) reported another situation in which I/S clays failed to reflect a major synsedimentary overthrust. Bruce (1984), in contrast, concluded that geologic age is not important to the reaction, and Bouchet *et al.* (1988) reported an increase in the illite proportions in the vicinity of even very minor veins and suggested only a different transformation mechanism.

Rock type, with its related porosity/permeability, also plays a role in the composition of I/S. Howard (1981), Smart and Clayton (1985), Boles and Franks (1979) and Eberly and Crossey (1989) all observed that the I/S clays tended to be much more expansible in sandstones than in adjacent shales. These data contrast with those of Ramseyer and Boles (1986) who found that I/S in shales tended to show a slightly higher content of smectite layers than I/S in closely-spaced sandstones. For paleotemperature evaluations only homogeneous mudstones are therefore assumed to give consistent results (Smart and Clayton, 1985).

Smectite diagenesis occurs simultaneously in time and space with the maturation of organic matter. Vitrinite reflectance is now considered one of the best parameters for defining the thermal maturity of organic matter, and certain critical I/S compositional ranges can be correlated with levels of organic maturity (Heroux *et al.*, 1979). The opinion is generally expressed, however, that clay minerals react much less readily to short-lived temperature increases than does organic matter (Środoń, 1979; Aoyagi and Asakawa, 1984).

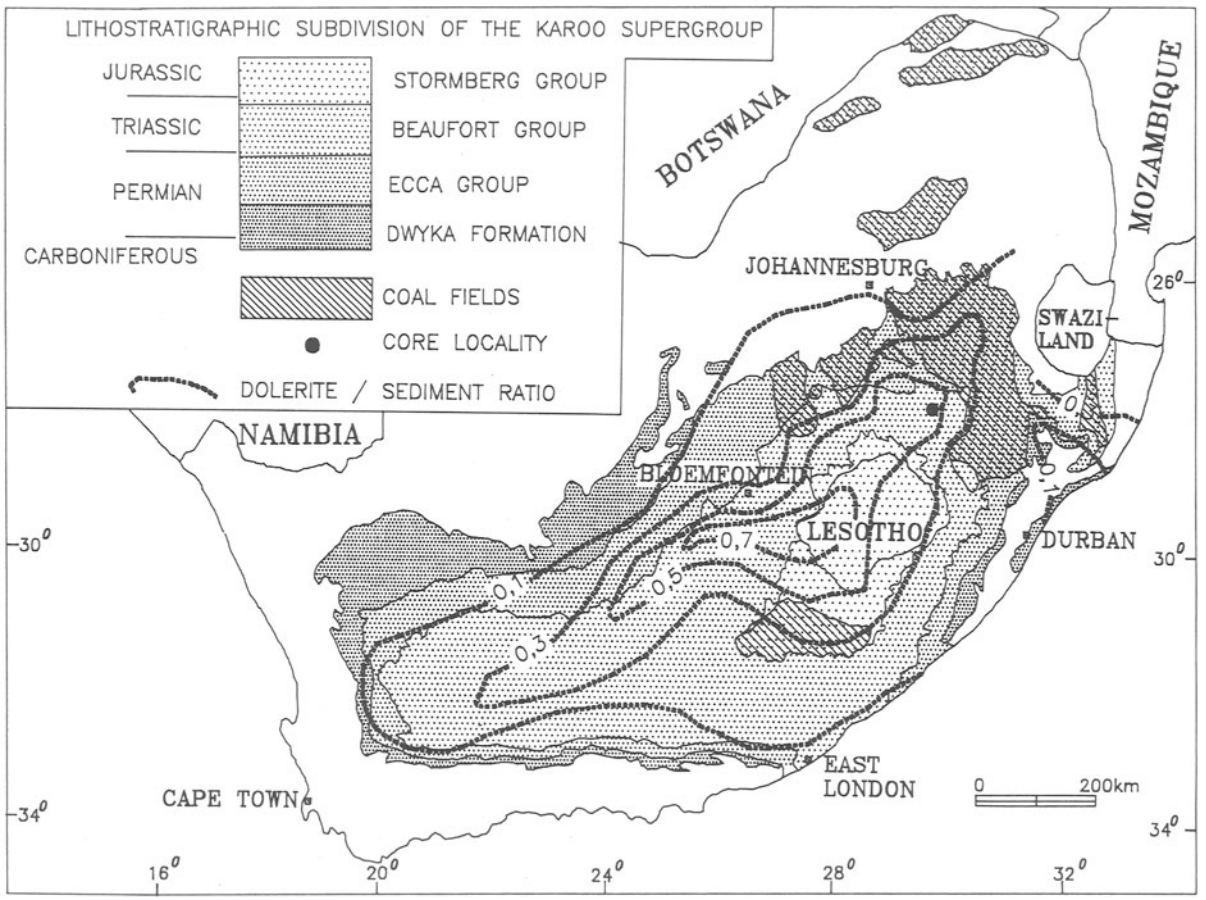

Figure 1. Great Karoo Basin with stratigraphic subunits, coalfields, dolerite/sediment ratios, and sample locality.

Comparatively few studies have attempted to document the nature of the clay fraction of Karoo sediments. Rowsell and De Swardt (1976) reported I/S from some borehole cores but failed to furnish compositional data. Heysteck (1954) described one example of a rectorite from the vicinity of a dolerite sill. No correlation between I/S composition and organic maturity levels has ever been attempted.

The paucity of data on clay mineral associations in the Republic of South Africa led to an investigation of several borehole cores transecting the Karoo strata. The aim was to discern the nature of the depositional environments (Bühmann and Bühmann, 1987). During this study, obvious temperature-dependent trends have been identified in the I/S composition in the vicinity of even minor dolerite sills (Bühmann, 1991). To quantify these trends, a lithologically complex sedimentary Permian sequence underlying dolerite sills was taken as an example. Correlation of I/S compositional variations with vitrinite reflectance data will also contribute to the knowledge of the time-duration parameter on the illitization reaction in contact aureoles, an environment from which few data are available. The study also provides information on lithology-related smectite illitization, for which contrasting findings are reported.

GEOLOGY

The Karoo Basin, which covers about half of the Republic of South Africa, accumulated sediments from the Late Carboniferous to the Jurassic. The post-sedimentary history of the Karoo strata is controlled by two major thermal regimes: diagenesis, largely related to burial-geosynclinal subsidence and local contact metamorphism in connection with the extrusion of basalt and the intrusion of dolerite sills and dikes. Results from organic maturity studies reveal a general increase in diagenesis from north to south (Rowsell and De Swardt, 1976; Smith and Whittaker, 1986).

The Karoo strata consists of a variable sequence of diamictite, arkosic sandstones, siltstones and carbonaceous mudstones, with economically significant coal seams in some formations and areas (Van Vuuren,

https://doi.org/10.1346/CCMN.1992.0400107 Published online by Cambridge University Press

1983). The lithostratigraphic subdivision, suggested by the South African Committee on Stratigraphy (1980) for Permian sediments, is given in Figure 1. Ecca Group sediments in the study region are subdivided into the Pietermaritzburg Formation, the Vryheid Formation, and the Volksrust Formation.

Variations in the mineralogical composition are commonly found within and between samples of the various lithologies (Rowsell and De Swardt, 1976; Bühmann and Bühmann, 1987). Overall the nonclay fraction contains quartz as a major constituent, varying proportions of K-feldspar and plagioclase, and occasionally carbonates, apatite and pyrite. The clay fractions consist of mica and chlorite in the main Karoo Basin (Rowsell and De Swardt, 1976). In the northern and north-eastern part of the basin, however, considerable proportions of illite/smectite interstratifications occur associated with mica and chlorite. Kaolinite consitutes the dominant clay mineral in the coal-bearing, predominantly fluvial part, which is situated at the northern fringes of the Karoo Basin (Figure 1; Bühmann and Bühmann, 1987).

Most of the Karoo sequence is gently dipping or virtually flat-laying, with successively higher strata being exposed inwards towards the Lesotho plateau (Figure 1). Karoo sediments have been subjected to burial diagenesis due to geosynclinal subsidence. Related temperatures range from about 60°C in the Orange Free State coalfield to approximately 180°C in the Vryheid coalfield and reached the stage of incipient greenschist metamorphic facies in the southern Cape (Rowsell and De Swardt, 1976; Smith and Whittaker, 1986; Saggerson and Turner, 1988). Post-burial modifications are controlled by the intrusion of dolerite sills and dikes, and by uplift and erosion.

The emplacement of basic magma in the form of intrusions (dolerite sills and dikes) and extrusions (Drakensberg basalt) during the Jurassic volcanic event over the whole subcontinent is responsible for local contact effects of relatively short duration. The intrusive sills vary in thickness from a few centimeters to several hundred meters. Dolerite/sediment-ratio maps reveal high ratios of 0.7 on the easternmost border of Lesotho and a gradual decrease to 0.1 in all directions (Figure 1).

The metamorphic effect of the dolerite intrusives on the Karoo strata has been studied predominantly in relation to maturity stages of coal. Thermal effects vary depending on proximity and thickness of the sills and dikes, but the initial temperature of the intrusion and its position in relation to the coal seam seem to be contributing factors (Smith and Whittaker, 1986).

During a mineralogical investigation of Karoo strata from seven borehole cores which formed part of a paleo-environmental study, characteristic trends were identified in the illite content of I/S in sediments on either side of dolerite intrusives.

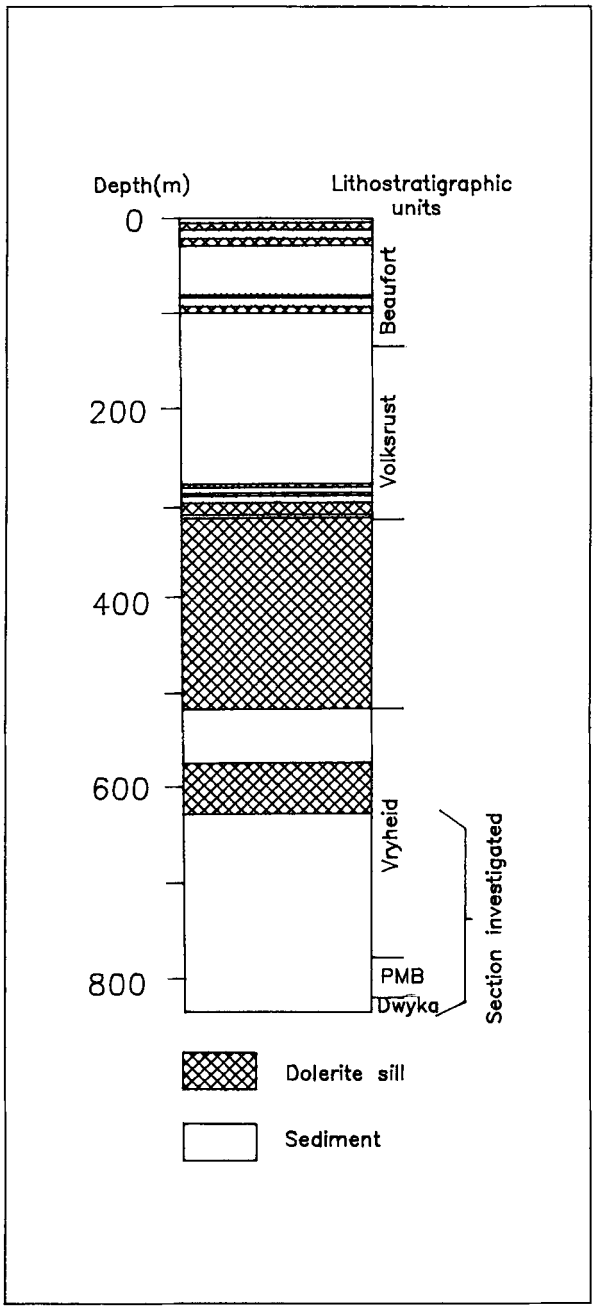

Figure 2. Lithostratigraphic subunits and dolerite/sediment relations of core SR1/75.

MATERIALS AND METHODS

Samples for the present investigations were derived from the SOEKOR research core SR1/75, obtained from the farm Strijd Plaats 237 in the Vrede district of the Orange Free State (Figure 1). The Karoo sedimentary rocks in the 838 m core are transected by nine dolerite sills, situated at the depths depicted in Figure 2. The study was confined to the section underlying the deepest dolerite sill (625–835 m; Figure 2). Samples

https://doi.org/10.1346/CCMN.1992.0400107 Published online by Cambridge University Press

were collected at varying intervals and cover the stratigraphic interval from Dwyka to most of the Vryheid Formation. Rowsell and De Swardt (1976) estimated burial-diagenetic temperatures of about 100°C for the study locality, based on the lowest CR (residual, non-volatile)/CT (total carbon) ratios of 0.73 after pyrolysis. The dolerite/sediment ratio is about 0.5.

A total of 120 samples was analyzed by means of X-ray diffractometry for semiquantitative bulk and clay mineral compositions. Analyses were carried out on a Philips XRD unit operated at 40 kV and 40 mA at a scanning rate of 1°2θ/min, using a graphite monochromator and CoKα radiation. Whole-rock random powder patterns were recorded from 3° to 75°2θ; oriented clay specimens from 2° to 35°2θ.

The samples were gently crushed and pulverized. Unoriented mounts were prepared by pressing the whole-rock powder against a rough filter paper. Semiquantitative estimates were based on peak-height percentages.

The pulverized clay fractions were dispersed ultrasonically and the <0.5-μm fractions concentrated by centrifugation. Calgon was used as a dispersing agent for a few samples (all pyrite-containing), where flocculation was a problem. Clay fractions were saturated with Mg by shaking in a 1 mol dm^{-3} chloride solution for 1 hour and left to equilibrate overnight. The flocculated clay was freed of excess salt by repeated centrifuge washings. Orientation of the clay was achieved by the suction-through method. Expansion tests were performed by solvation with ethylene glycol and glycerol (vapor at 60°C and 90°C, respectively; Novich and Martin, 1983) and intercalation with hydrazine (*in vacuo* for two days).

Clay mineral nomenclature follows AIPEA recommendations (Bailey, 1980, 1982). Differentiation between chlorite and kaolinite is based on hydrazine intercalation (Range *et al.*, 1969). Layer proportions and ordering of I/S were determined from Mg-saturated, ethylene glycol-solvated specimens according to the quantification curves of Tomita *et al.* (1988). Where peaks were not sufficiently resolved, the criteria of Reynolds and Hower (1970) were applied using the spacing of the 5–5.6 Å reflection, with supplements for R = 1 by the presence of a superlattice reflection and for R = 0 by the shape of the 17 Å peak. Ordering was classified in "Reichweite" notations as defined by Reynolds and Hower (1970) and Reynolds (1980), and as illustrated by Tomita *et al.* (1988). Vitrinite reflectance measurements were conducted on 13 carbonaceous mudstone samples to quantify potential temperature-related trends via levels of organic maturity.

RESULTS

Whole-rock mineralogy

The qualitative and semiquantitative composition of the whole-rock samples reflected semiarkosic sand-

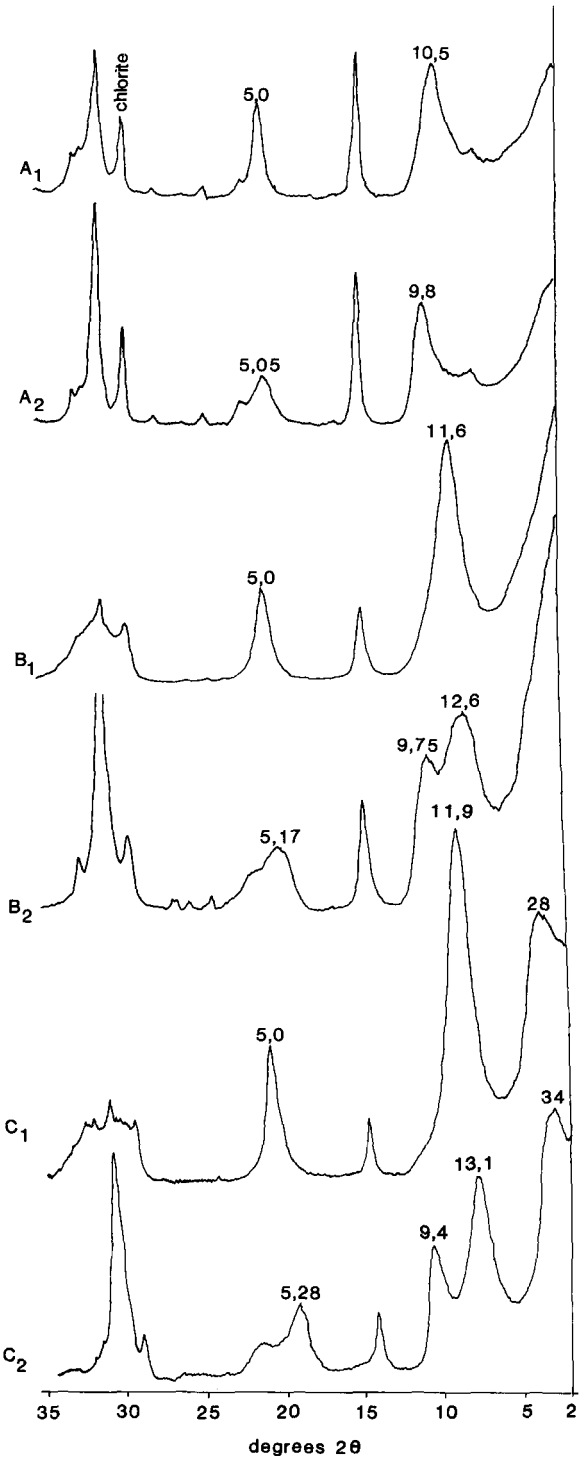

Figure 3. Representative X-ray traces of the <0.5-μm fractions from section a (625.8 m–677.7 m; oriented specimen). (A) Sample from 627.0 m depth A_1: Mg-sat., air dried A_2: Mg-sat., ethylene glycol solvated. (B) Sample from 638.1 m depth B_1: Mg-sat., air dried B_2: Mg-sat., ethylene glycol solvated. (C) Sample from 665.0 m depth C_1: Mg-sat., air dried C_2: Mg-sat., ethylene glycol solvated.

https://doi.org/10.1346/CCMN.1992.0400107 Published online by Cambridge University Press

Table 1. Trends in I/S composition in relation to profile depth, lithology, associated clay and Ca-bearing minerals, and vitrinite reflectance.

Depth (m)	Lithology	Reichweite notation	% Illite in I/S	Add. clay minerals in <0.5-μm fraction	% Calcite + dolomite + apatite	RoV (max) %
625.8	mst	R = 3	89	chl;		
627.0	f, sst/cb	R = 3	95	chl	43	
632.6	f, sst	R = 3	91	chl	10	
636.0	siltst/mst, lam	R = 3	93	*chl*	2	
637.4	mst	R = 3	87	chl		1.93
638.1	mst	R > 1	82	chl		
639.0	mst	R = 2?	85	chl; mi		
640.0	mst/siltst	R = 2 + 1	83	chl	14	
640.05	sst	R = 3	87	chl		
641.6	mst	R = 1	81	py; kao; chl; mi		
642.1	mst	R > 1	81	py; kao; chl; mi		
642.8	siltst	R > 1	86	chl		
645.2	mst	R = 1	89	chl		
652.0	mst	R = 1	80	chl		
657.0	mst	R > 1	82	chl		2.70
657.5	mst	R = 1 + 2	86	chl	11	
663.8	sst	R = 1 + 2	85	mi; chl	5	
665.0	m, sst	R = 1	72	chl		
665.5	sst	R = 1	72	chl	6	
669.5	sst	R = 1	82	chl		
672.0	mst	R = 1 + 2	65	chl	9	
672.4	sst, flas	R = 1	89	chl		
675.5	f–m, sst	R = 1	64	chl		
677.7	mst	R = 1	85	chl; mi		
678.2	mst	R = 1	65	chl; mi		1.25
680.0	mst/sst, lam	R = 1	65	chl	8	
682.6	m, sst	R = 1	66	chl		
684.5	siltst, lam	R = 1	65	chl		
686.3	bio sst	R = 1	63	*chl*	20	
688.6	lam. siltst/mst/cb	—	—	*chl*; mi	45	
690.3	siltst	R = 1	65	chl		
692.0	lam f, sst/mst	R = 1	79	chl; mi	4	
693.6	mst	R = 1	65	chl; mi		
695.2	f–m, sst	R = 1	65	chl	3	
697.9	mst	R = 1	72	*chl*	13	
699.5	lam mst/siltst	R = 1	65	chl		
704.0	mst	R = 1	49?	*chl*; mi		1.12
706.5	mst/cb		—	corrensite	48	
707.5	lam mst/siltst	R = 1	65	kao; chl		
708.6	lam mst/siltst	R = 1	65	kao; chl		
710.0	lam. siltst/mst	R = 1	62	kao; chl		
711.6	mst	R = 1	59	kao; chl		
713.6	flas sst	R = 1	65	kao		
714.8	mst	R = 1	63	kao; chl		1.20
716.0	mst	R = 1	68	*kao*		
717.6	siltst	R = 1 + 0	68	kao	4	
718.5	cb	—	—	*chl*; mi; kao	64	
720.0	mst	R = 1 + 0	67	mi; kao; chl		
721.6	lam siltst/mst	R = 1 + 0	55	kao; chl; mi		
722.8	flas sst	R = 1	60	*chl*; kao; mi	13	
724.0	bio sst;	R = 1	66	chl; kao		
725.3	mst	R = 1	65	kao; mi; chl		
727.0	mst	R = 1	58	kao; mi; chl	2	
730.0	mst	R = 1	57	mi; kao; chl	2	
732.0	mst	R = 1	58	*kao*; mi; chl	3	
733.6	mst	R = 1	66	kao; mi; chl		
735.0	flas siltst/mst	R = 1	65	kao;		
736.0	mst	R = 1	66	*kao*; mi	2	1.25
737.4	mst	R = 1	66	kao		
738.6	mst	R = 0 + 1	65	mi; chl; kao		
738.8	mst	R = 0 + 1	66	chl; mi; kao	11	
739.0	mst	R = 1	60	*kao*; mi		1.29
740.3	siltst/mst	R = 1	66	*chl; mi*; kao		
740.6	mst	R = 1	65	*kao; chl*; mi		

https://doi.org/10.1346/CCMN.1992.0400107 Published online by Cambridge University Press

Table 1. Continued.

Depth (m)	Lithology	Reichweite notation	% Illite in I/S	Add. clay minerals in <0.5-μm fraction	% Calcite + dolomite + apatite	RoV (max) %
742.3	sst, pyritic	?	66(?)	kao; chl; mi		
742.6	m, sst	R = 1	65	kao; chl	4	
743.2	flas, sst	R = 1	67	chl; kao		
744.6	flas, sst	R = 1	63	kao; chl	3	
747.0	siltst	R = 1	66	chl; mi; kao		
749.0	lam sst	R = 1	58	*kao*; chl; mi		
751.5	flas sst/siltst	R = 1	54	chl; kao	1	
753.0	siltst	R = 1	61	kao; chl; mi		
756.0	m–c, sst	R = 1	63	*kao; chl*; mi	10	
758.0	mst	R = 1	66	*kao; chl*; mi	5	1.16
759.8	sst	R = 1	64	kao; chl; mi		
760.6	mst	R = 1	58	chl; kao; mi	3	
762.0	mst	R = 1	66	*kao; chl*; mi		
763.0	mst	R = 1	66	*kao; chl; mi*		
765.0	lam siltst/mst	R = 1	63	*kao*; mi; chl		
767.0	lam mst/siltst	R = 1	66	*kao*; mi; chl		
768.5	lam mst/siltst/sst	R = 1	58	*kao*; mi	4	
772.5	lam siltst/mst	R = 1	60	*kao*; chl; mi	20	
774.0	siltst/mst, bio	R = 1	59	*kao; chl*; mi		
775.0	flas sst/siltst/mst	R = 1	58	*kao*; mi		
776.8	mst	R = 0	60	*kao; chl; mi*		
778.5	mst	—	—	*kao*; chl; mi	19	
780.0	mst	R = 0	58	*kao; chl; mi*		1.07
781.7	mst	R = 1	63	*kao*; chl; mi		
783.0	flas sst	R = 1 + 0	58	*kao*; chl; mi	26	
Pietermaritzburg Formation						
785.0	siltst	R = 0 + 1	45	*kao*; chl; mi		
786.5	mst	R = 0	52	*kao*; mi; chl		1.17
788.2	mst	R = 0	40	kao; mi; chl	3	
789.4	siltst	R = 0 + 1	50	mi; kao	6	
790.6	siltst	R = 0 + 1	41	mi; kao	7	
791.8	siltst	R = 0	39	mi; kao; chl		
793.0	siltst	R = 0 + 1	50	chl; mi; kao		1.42
793.5	mst	R = 0	52	kao; chl; mi	1	
793.6	mst-siltst.	R = 0	42	mi; kao; chl		
795.2	mst	R = 0	40	kao; mi;		
796.4	mst	R = 0	50	kao; mi		
797.7	siltst	R = 0 + 1	50	mi; kao; chl	4	
798.9	mst	R = 0	41	mi; chl; kao	3	
806.0	mst	R = 0	39	chl; kao; mi	2	
808.0	siltst	R = 0 + 1	45	kao; chl; mi	2	
810.0	mst	R = 0	50	chl; mi; kao		
812.0	mst	R = 0	35	chl; mi; kao		1.44
815.2	mst	R = 0	30	chl; kao; mi		
818.0	mst	R = 0	40	chl; mi; kao		
821.0	mst	R = 0	40	chl; mi; kao		
822.0	mst	R = 0	49	chl; mi; kao		
823.0	mst	R = 0	42	chl; mi; kao		1.52
825.0	mst	R = 0 + 1	50	mi; chl; kao		
827.0	siltst	R = 0 + 1	50	chl; mi; kao		
827.8	mst	R = 0	42	*kao*; mi; chl		
Dwyka Formation						
828.0	conglomerate	R = 1 + 0	59	*kao*; mi; chl		
829.5	f sst	R = 1	65	kao; chl; mi		
831.5	f-m sst	R = 1	62	kao; mi; chl		
835.8	diamictite	R = 1	65	*chl*; mi		
837.6	diamictite	—	—	*chl*	13	
837.8	diamictite	R = 1 + 0	59	*chl*		
Greenstone						

mst: dark-grey to black, carbonaceous mudstone; siltst: siltstone; sst: white to grey sandstone; f: fine-grained; m: medium-grained; c: coarse-grained; bio: bioturbated; lam: laminated; flas: flaser; cb: carbonate; mic: micaceous; chl: chlorite; kao: kaolinite; mi: mica; py: pyrophyllite.

https://doi.org/10.1346/CCMN.1992.0400107 Published online by Cambridge University Press

stone, siltstone, and mudstone lithology. Quartz was generally the dominant nonclay phase. K-feldspar and plagioclase were present in varying proportions in most samples with no apparent depth relation. Carbonates, apatite, or pyrite constituted a major phase in some horizons. Carbonates included siderite, calcite, dolomite, and ankerite, in order of decreasing abundance. Two samples each contained pyrophyllite and apophyllite. Two or more of the following phyllosilicates could be identified from the powder patterns: mica, chlorite, illite/smectite, and kaolinite. Mica is predominantly detrital as indicated by its large particle size of a few millimeters. The similarity in the qualitative and average quantitative composition of the detrital nonclay fraction gives evidence that source area characteristics varied little with time.

Clay mineralogy (<0.5 μm)

All phyllosilicates were dioctahedral. Consistent stratigraphic trends were apparent in the relative abundance of certain clay minerals. These differences were particularly pronounced in the 2:1 phyllosilicates-versus-kaolinite ratio, and were not lithology-related. Marine sections (Pietermaritzburg Formation) were dominated by 2:1 layer silicates, while fluvial deposits (parts of the Vryheid Formation) contained abundant kaolinite (Table 1). Compared to the whole-soil composition, mixed-layer I/S was considerably enriched in the <0.5-μm fraction, mainly at the expense of mica. Mica, chlorite and kaolinite were generally accessory minerals. Two samples contained pyrophyllite.

Compositional trends in I/S as a function of depth and lithology are depicted in Table 1. The I/S passes through a sequence of transformations with increasing distance from the sill contact. Variations in I/S composition spanned the range from R = 3 interstratifications with about 95% illite to R = 0 with as much as 70% of expandable layers (Table 1). All samples containing >86% illite layers showed moderate to strong R = 3 order. R = 1 I/S had on average 64.4% and random I/S had 45.6% illite.

On the basis of I/S mineralogy the sequence could be subdivided into four sections with increasing distance from the nearest dolerite sill contact.

Section 1; 625 m–678.2 m depth. In this lithologically-complex sequence there was a considerable down-section decrease in the proportions of illite from 95% in a R = 3 stacking arrangement in close vicinity to the sill to R = 1 with 65% at a depth of 678.2 m (Table 1). Representative profiles are shown in Figure 3. The sample at 627.0 m is represented in the Mg-saturated, air-dried scan by peaks at 10.5 Å and 5.0 Å. Glycolation led to a decrease in the first reflection to 9.8 Å, with a shoulder toward lower 2θ values. The spacing of the second peak increased to 5.05 Å. The shape of the first reflection and the position of the second indicate illite proportions of about 95%. The pattern closely resembles the theoretical Reichweite R = 3 ordering. I/S is associated with major amounts of chlorite. The sample from 638.1 m depth is represented in the Mg-saturated, air-dried scan by the 11.6 and 5.0 Å peaks. Glycolation caused splitting of the first basal reflection into 12.6 Å and 9.75 Å peaks, and migration of the 5 Å reflection to 5.17 Å. These peaks are indicative of an ordered I/S and represent combinations from $002_{27}/001_{10}$, $003_{27}/001_{10}$ and $005_{27}/002_{10}$, respectively. Peak positions indicate an illite proportion of 82%. The sample from 665.0 m depth is characterized by a superlattice reflection at about 28 Å, and peaks at 11.9 Å and 5.0 Å in the Mg-saturated, air-dried state. Treatment with ethylene glycol gave rise to diffraction lines at 34, 13.1, 9.4, and 5.28 Å. These peak positions indicate that the structure is a R = 1 interstratification with an illite proportion of about 70% (Tomita *et al.*, 1988). The sample contained minor amounts of chlorite.

The systematic decrease in the proportion of illite in the I/S with increasing distance from the nearest dolerite intrusive over a distance, similar to the thickness of the nearest dolerite sill, is evidence that the thermal alteration is dolerite-derived. Two mudstone samples (641.6 m and 642.1 m) contain pyrophyllite associated with kaolinite, I/S, chlorite, and mica (Figure 4).

Section 2; 678.2 m–785.0 m depth. Almost all samples in this lithologically-variable strata are composed of rectorite in which the smectite proportions increased only slightly from about 35% to 40%. XRD tracings of the ethylene glycol-solvated <0.5-μm fractions are typified by Figure 5, which shows the superlattice and double-peak characteristics of ordered R = 1 I/S. An observation, which also applies to the above described section, is that differences in I/S composition and stacking arrangements between different lithologies are insignificant. Mudstone layers displayed less sharp peak characteristics than sandstone layers (Figures 5b, c), but varied within almost identical compositional ranges (62.3% and 63.1%, respectively). Most samples contained chlorite, kaolinite, and mica (Table 1).

Section 3; 786.5 m–828.0 m depth. This uniform, carbonaceous mudstone/siltstone strata was dominated

←

I/S is the dominant phase in the <0.5-μm fraction, unless otherwise indicated by italics. Additional clay phases are depicted in order of decreasing abundance.

https://doi.org/10.1346/CCMN.1992.0400107 Published online by Cambridge University Press

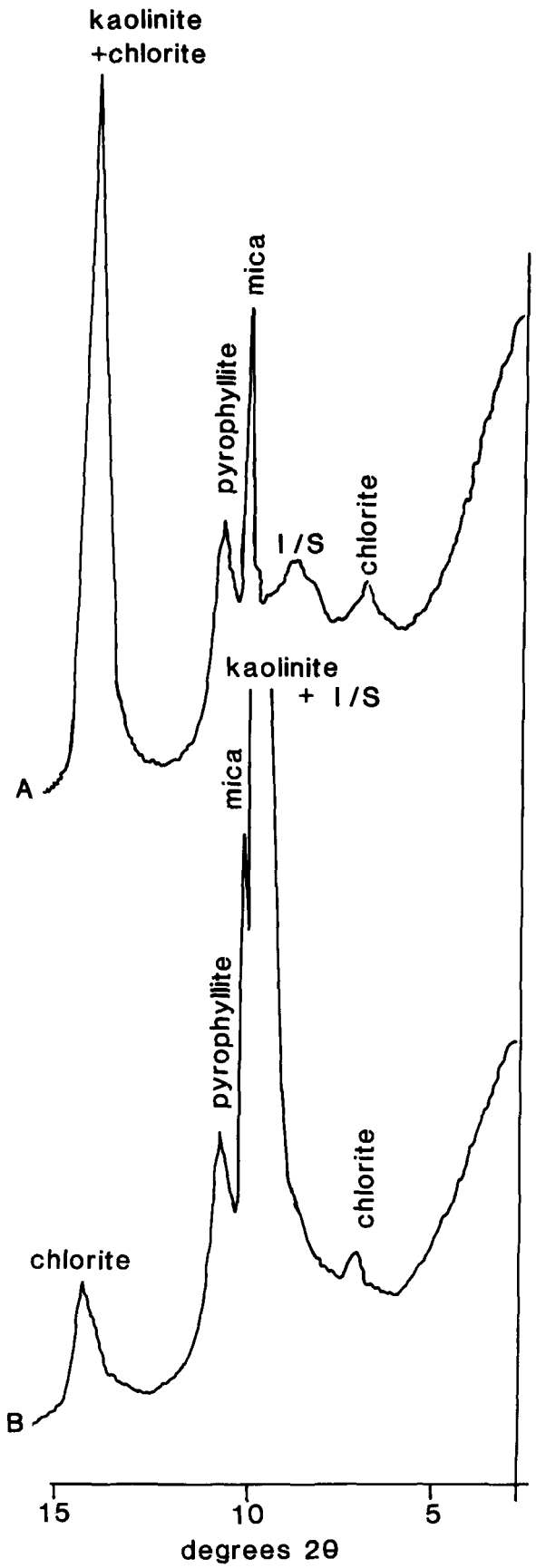

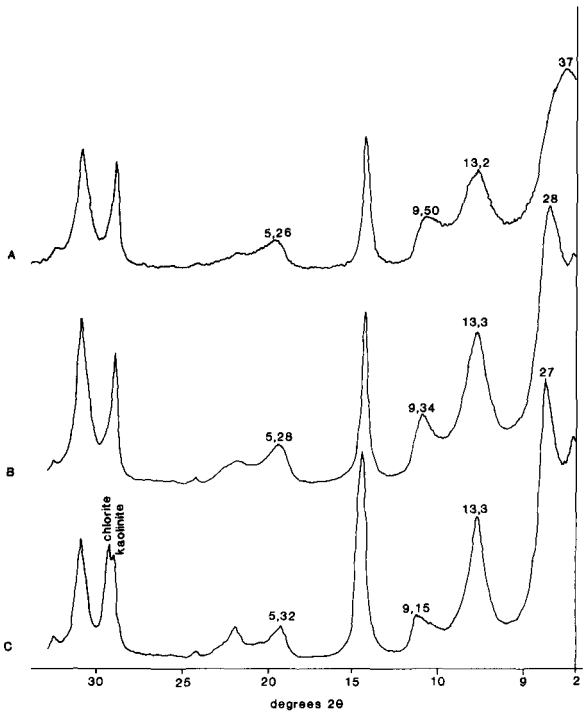

Figure 5. Representative X-ray traces of the <0.5-μm fractions (oriented specimen; Mg-sat., ethylene glycol solvated) from section b (678.2 m–783.0 m). (A) Mudstone (708.6 m); (B) sandstone (710.0 m); (C) sandstone (760.6 m).

by random (R = 0) I/S (Figure 6), unambiguously identified by the presence of a 17 Å reflection after glycolation, according to the criteria of Reynolds and Hower (1970). Most siltstones contained small amounts of ordered structures associated with the random ones, while almost all mudstone samples displayed random stacking characteristics only (Table 1). The transition from section 2 to 3 occurred abruptly from 783.0 m to 785.0 m, a depth that reflects the transition from the Vryheid to the Pietermaritzburg Formation (Table 1). In this section lithology seemed to play a minor part in the illite proportions, with siltstones having on average 46.3% illite, and mudstones 42.2%.

Section 4; 828 m–838 m depth. This section was composed of Dwyka diamictite and fine- to medium-grained sandstone and conglomerates. The I/S displayed R = 1 stacking order and illite proportions of 59–65% (Table 1); almost identical to that of section 2. Calcite-rich layers, despite their decreased permeability and counter ion presence, were characterized by a similar I/S composition as the equivalent carbonate-free li-

←

Figure 4. X-ray traces of the sample from 641.6 m depth (oriented specimen, <0.5-μm fraction). (A) Mg-sat., air dried; (B) Hydrazine intercalated.

https://doi.org/10.1346/CCMN.1992.0400107 Published online by Cambridge University Press

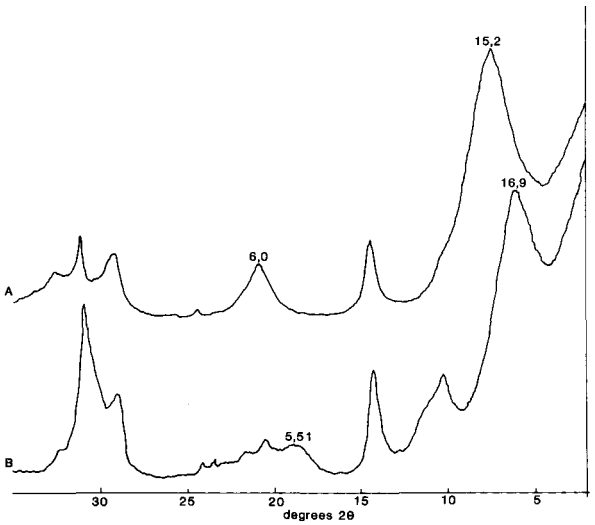

Figure 6. Representative X-ray traces of the <0.5 μm fraction of the sample from 827.0 m depth (oriented specimen). (A) Mg-sat., air dried; (B) Mg-sat., ethylene glycol solvated.

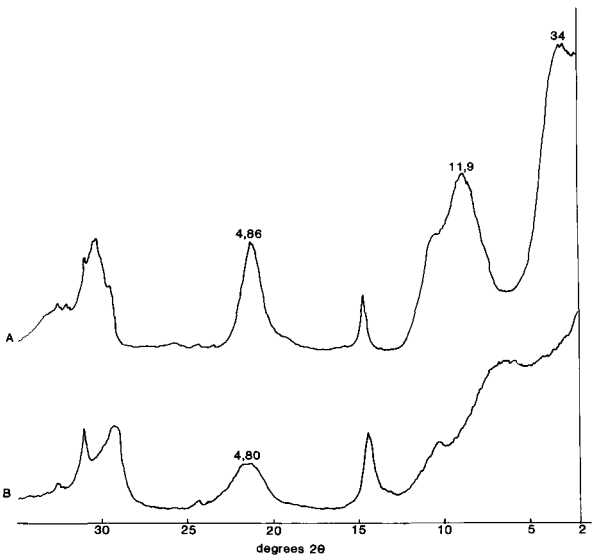

Figure 7. X-ray traces of glycerol-solvated, oriented specimen of the <0.5-μm fraction of (A) R = 1 (665.0 m), and (B) R = 0 (827.0 m) I/S interstratifications. X-ray traces of the samples after ethylene glycol solvation are depicted in Figures 3 and 6, respectively.

thologies. High calcite contents, however, led to the formation of chlorite instead of I/S. K-bearing minerals did not disappear systematically with the development of illite layers. Glycerol solvation produced spacings characteristic of a monolayer formation in all ordered stacking arrangements, and both monolayer and bilayer formation in random structures (Figure 7).

Vitrinite reflectance

Every sample showed two or more populations of vitrinite, as far as rank was concerned, because each sample contained more than one sedimentary layer. Trends in the maximum reflectance of reactive vitrinite with increasing profile depth are presented in Table 1. Maximum vitrinite reflectance values were highest (with 1.93 and 2.70) in close contact to the intrusive where I/S displayed R > 1 ordering. In section 2 of the profile, where R = 1 I/S dominates, vitrinite values varied within the narrow range 1.07–1.29. The massive mudstone sequence of the Pietermaritzburg Formation, dominated by R = 0 interstratifications, was characterized by vitrinite reflectance values around 1.4.

DISCUSSION

While the thermal implications of the illitization reaction are well-documented from burial-diagenetic sequences, there is a paucity of data from contact metamorphic environments (Nadeau and Reynolds, 1981; Smart and Clayton, 1985; Aaron and Lee, 1986). The objective of this study, therefore, was to determine the thermometamorphic effect of dolerite intrusions on the composition of interstratified I/S and to correlate it with vitrinite reflectance data. A second aim was to establish the influence of lithology on the I/S composition, for which contrasting information is available.

Thermal history obviously exerted the primary control. Over a distance of only 210 m, the sequence inversely duplicates trends observed in burial-diagenetic sequences over distances of several thousands of meters. Mineralogical maturity levels are reflected by smectite-to-illite ratios, and in two samples (641.6 and 642.1 m) by the occurrence of pyrophyllite.

The effect of igneous intrusives on sedimentary rocks depends primarily on the thickness of the intrusive body. The distance over which changes take place may vary considerably, however. Contact aureoles in the vicinity of dolerite sills are reported by Hagelskamp (1988) to average three times the thickness of the intrusive body, while Rowsell and De Swardt (1976) found "some metamorphic effect" to persist over a distance of twice the width of the sill. Dennis *et al.* (1982) measured changes in vitrinite reflectance at distances of one to two times the sill thickness, and Simoneit *et al.* (1981) only to a distance of about half the sill thickness. In 1974, Connan *et al.* (cited by Rowsell and De Swardt, 1976) even showed for the northern Karoo, that sills, which are usually not very thick, did not cause any metamorphism at all.

The systematic decrease in the illite proportions in the I/S with decreasing proximity from the nearest dolerite sill contact from 95% to 65% (625.8 m–678.2 m) is evidence that the thermal alteration is dolerite-derived. Vitrinite reflectance values are highest in this contact aureole section, but do not vary systematically with depth. They suggest a similar distance of thermal impact influence, however.

https://doi.org/10.1346/CCMN.1992.0400107 Published online by Cambridge University Press

The temperature that marks the transition of R = 1 to R > 1 I/S is of interest in paleothermometry analysis. Glasmann *et al.* (1989) correlated the occurrence of long-range I/S with temperatures of 150–160°C, and Velde (1985) the R = 1-to-R = 3 transition with 180°C. Hower *et al.* (1976), too, reported the onset of R = 3 I/S formation at temperatures of 180°C in the Gulf Coast burial sequences. In the present study, vitrinite values of 1.9 and 2.7, which attest to temperatures of about 160°C and 180°C, are associated with R = 3 and R > 1 interstratifications having about 13% and 18% smectite, respectively. The R > 1 interstratifications, which formed by contact metamorphism, obviously required similar temperatures as do equivalent structures from geothermal or burial-diagenetic environments.

Pyrophyllite may also be taken as a paleotemperature indicator. Laboratory experiments on the stability of pyrophyllite have established a lower limit at 270°C and 1–2 kb (Hemley *et al.*, 1980). In natural environments, however, transformation of kaolinite to pyrophyllite occurs at lower temperatures. Frey (1978) reported pyrophyllite from sediments that were subjected to temperatures of only 200°C. In coal measures of Japan, onset of pyrophyllite formation is even correlated with temperatures as low as 165°C derived from vitrinite reflectance values of 2.6 (Iijima and Matsumoto, 1982). A $RoV_{(max)}$ of 2.7, recorded in the present study in a sample close to the pyrophyllite-bearing layer, correlates very well with organic maturity data from the coal fields of Japan. Therefore, time duration will not have been a governing factor in the contact-metamorphic alteration of the Karoo sedimentary rocks.

The second temperature of interest concerns the change from random to ordered I/S stacking arrangements. Velde (1985) noted that the transition took place at about 80°C in high geothermal sequences, and at 50°–80°C in deep drillholes. Pearson and Small (1988) correlated the disappearance of random I/S with temperatures of 93°C, while Glasmann *et al.* (1989) found ordering to develop over a temperature range of 80°–110°C. Hower *et al.* (1976) infer a temperature of formation of 100°C for R = 1 I/S with >60% illite. In the present mixed-lithology section 2 (687.2 m–785.0 m), R = 1 interstratifications with on average 63% illite are associated with vitrinite reflectance levels of 1.0–1.2, which attest to a paleotemperature of about 100°C. This inferred temperature compares well with that of Hower *et al.* (1976), Pearson and Small (1988), and Glassman *et al.* (1989).

When using I/S compositional criteria for paleotemperature evaluation, the absence of ordered stacking arrangements in most of the Pietermaritzburg Formation mudstones indicates paleotemperatures below 80°C (Velde, 1985), and accordingly, significantly below the ~130°C, established via vitrinite reflectance measurements. There is no obvious reason for the association of random I/S structures having ~45% illite with vitrinite reflectance values that are higher than those associated with ordered R = 1 arrangements having ~62% illite.

Organic maturation indices such as vitrinite reflectance are generally reported to be superior to I/S as paleotemperature indicators (Środoń, 1979; Aoyagi and Asakawa, 1984; Smart and Clayton, 1985; Tissot *et al.*, 1987). If this assumption is correct, we have to postulate the existence of a temperature source that has led to increased vitrinite reflectance in the mudstone sequence but failed to lead to enhanced illitization. There is no evidence for the presence of such a source, however. Mudstones from the Pietermaritzburg Formation disintegrate much more readily than those from the overlying Vryheid Formation; an indicator of a lower degree of inorganic maturity. The transition between the two parts of the profile occurs abruptly and coincides closely with the lithologic boundary. The Dwyka sandstone section, underlying the mudstone sequence, is also too similar in I/S characteristics to the mixed-lithology section overlying it, for a temperature source in the greenstone section to be postulated. The author is positive that the existence of a dolerite sill influencing Pietermaritzburg sediments exclusively is unlikely. Two factors besides lithology differ between the two sequences: 1) The Pietermaritzburg Formation strata contains considerably more I/S than do mudstones from the Vryheid Formation, which are dominated by kaolinite. This difference in matrix mineralogy could account for differences in organic maturity. A possible enhanced thermal alteration of the organic matter caused by thermocatalytic properties of the smectite is possible, as suggested by Huizinga *et al.* (1987). 2) The depositional environment was different. Shales from the Pietermaritzburg Formation were deposited in a marine setting, whereas the Vryheid Formation mixed lithology is indicative of a fluvial-to-deltaic environment (Van Vuuren, 1983). A different type of organic matter, more readily thermally converted, could be the cause of the contrasting vitrinite data. Present data do not provide conclusive evidence in support of any of the possible interpretations.

The distance of the thermometamorphic influence relative to the dolerite sill thickness is difficult to evaluate. Based solely on trends in I/S compositions, and prior to conducting vitrinite reflectance measurements, the author was strongly inclined to interpret the entire sequence in one of two ways: 1) The whole sequence developed in response to a thermal gradient associated with the major sill, with only the uppermost section (625.8 m–678.2 m) being influenced by the deepest sill. The influence distance of the thermal impact associated with the 200 m-thick intrusive would then have been slightly more than the sill thickness, and the extent of the contact aureole well within the reported ranges of thermal influence. The lack of any significant variation

in I/S composition within section 2 would then be difficult to explain, however. 2) Random stacking arrangements in the massive mudstone part, and R = 1 I/S in the mixed-lithology section 2 of the core both reflect a burial-diagenetic history. In this case, lithology would play a major part in the illitization. Mixed-lithology sediments in which minor mudstone layers occur interbedded with sandstones and siltstones would be associated with less expansible I/S than massive mudstone facies. Should the thermal gradient in case 2 be derived from the lower sill only, it would extend over a distance similar to the width of the intrusive. If the major sill constituted the main temperature source, however, the timing of the intrusions relative to each other is of importance. In the case of the deepest sill postdating the major one, the distance of contact metamorphism would extend to about half of the sill thickness, or otherwise to a distance ¾ of the intrusive width. In any case, the extent of the contact aureole would also be within the reported ranges of thermal influence. Vitrinite reflectance measurements, however, do not support this interpretation. No satisfactory explanation for the discrepancy between organic and inorganic maturity data can be offered.

The availability of potassium is important to the reaction. Nadeau and Reynolds (1981) found that the percentage of illite layers in I/S was lower in calcareous than in noncalcareous environments. These findings are supported by hydrothermal experiments that show that the ratio of K to Ca to Mg is particularly important, with the divalent ions inhibiting the smectite-to-illite reaction (Roberson and Lahann, 1981; Inoue, 1983). In the present study the high contents of Ca-bearing minerals (calcite, dolomite, apatite) promoted transformation of smectite into chlorite rather than illite, while small calcite proportions had no influence on the I/S mineralogy.

CONCLUSIONS

Alteration of vitrinite and the progressive illitization of I/S occur simultaneously and reflect thermal gradients in the vicinity of dolerite sills. Time duration cannot be regarded a governing factor for the illitization reaction in Karoo sedimentary rocks. Comparing similar depth levels, no difference could be established in I/S compositions between sandstone and mudstone in the mixed-lithology section. In the massive mudstone/siltstone part of the core, however, siltstones show a higher regularity in I/S ordering, and slightly higher illite proportions than do equivalent mudstones. Carbonate-rich layers vary within a similar I/S compositional range, but contain significantly more chlorite. R > 1 interstratifications are associated with pyrophyllite and maximum vitrinite reflectances of 1.9–2.7, while R = 1 structures with on average 63% illite show vitrinite reflectance values around 1.1. Random I/S, however, occurs in samples with a vitrinite content of about 1.4.

I/S may reflect temperature trends better than vitrinite reflectance.

ACKNOWLEDGMENTS

Core samples were made available through the courtesy of the Geological Survey. The author is indebted to Mr. H. J. Roux, ISCOR Ltd. RSA, for conducting vitrinite reflectance measurements.

REFERENCES

Aaron, J. L. and Lee, M. (1986) K/Ar systematics of bentonite and shale in a contact metamorphic zone, Cerrillos, New Mexico: *Clays & Clay Minerals* **34,** 483–487.

Aoyagi, K. and Asakawa, T. (1984) Palaeotemperature analysis by authigenic minerals and its application to petroleum exploration: *Amer. Assoc. Petrol. Geol. Bull.* **68,** 903–913.

Bailey, S. W. (1980) Summary of recommendations of AIPEA nomenclature committee: *Clays & Clay Minerals* **28,** 73–78.

Bailey, S. W. (1982) Nomenclature for regular interstratifications: *Clay Miner.* **17,** 243–248.

Boles, J. R. and Franks, S. G. (1979) Clay diagenesis in Wilcox sandstones of Southwest Texas: Implications of smectite diagenesis on sandstone cementation: *J. Sed. Petrol.* **49,** 55–70.

Bouchet, A., Proust, D., Meunier, A., and Beaufort, D. (1988) High-charge to low-charge smectite reaction in hydrothermal alteration processes: *Clay Miner.* **23,** 133–146.

Bruce, C. H. (1984) Smectite dehydration—Its relation to structural development and hydrocarbon accumulation in northern Gulf of Mexico Basin: *Amer. Assoc. Petrol. Geol. Bull.* **68,** 673–683.

Bühmann, C. (1991) Clay mineralogical aspects of thermally induced parent material discontinuity. *Appl. Clay Sci.* **6,** 1–19.

Bühmann, C. and Bühmann, D. (1987) Sedimentary petrology of coal-bearing Ecca sediments (final report; unpubl.): University of Natal, Pietermaritzburg, 27 pp.

Dennis, L. W., Maciel, G. E., Hatcher, P. G., and Simoneit, B. R. T. (1982) ^{13}C nuclear magnetic resonance studies of kerogen from Cretaceous black shales thermally altered by basaltic intrusions and laboratory simulations: *Geochim. Cosmochim. Acta* **46,** 901–907.

Eberly, P. O. and Crossey, L. J. (1989) Compositional variation in clay mineral fractions of fine- and coarse-grained units in Westwater Canyon Member (Morrison Formation, San Juan Basin, New Mexico). *Amer. Assoc. Petrol. Geol. Bull.* **73,** p. 1154.

Frey, M. (1978) Progressive low-grade metamorphism of a black shale formation, Central Swiss Alps, with special reference to pyrophyllite and margarite bearing assemblages: *Jour. Petrology.* **19,** 95–135.

Glasmann, J. R., Larter, S., Briedis, N. A., and Lundegard, P. D. (1989) Shale diagenesis in the Bergen High area, North Sea: *Clays & Clay Minerals* **37,** 97–112.

Hagelskamp, H. H. B. (1988) The effect of dolerite intrusions on the quality of coal: *Extended abstracts, Geocongress '88,* University of Natal, Durban, 219–222.

Hemley, J. J., Monteya, J. W., Marinenko, J. W., and Luce, R. W. (1980) Equilibria in the system Al_2O_3–SiO_2–H_2O and some general implications for alteration mineralization processes: *Econ. Geol.* **75,** 210–228.

Heroux, Y., Chagnon, A., and Bertrand, R. (1979) Compilation and correlation of major thermal maturation indicators: *Amer. Assoc. Petrol. Geol. Bull.* **63,** 2128–2144.

Heysteck, H. (1954) Some hydrous micas in South African clays and shales: *Miner. Mag.* **31,** 337–355.

Hoffman, J. and Hower, J. (1979) Clay mineral assemblages as low grade metamorphic geothermometers: Application to the thrust faulted disturbed belt of Montana, USA: in *Aspects of Diagenesis,* P. A. Scholle and P. R. Schluger, eds., *Soc. Econ. Paleontol. Mineral. Spc. Publ.* **26,** 55–79.

Howard, J. J. (1981) Lithium and potassium saturation of illite-smectite clays from interlaminated shales and sandstones: *Clays & Clay Minerals* **29,** 136–142.

Hower, J., Eslinger, W. V., Hower, M., and Perry, E. A. (1976) Mechanism of burial metamorphism of argillaceous sediments: I. Mineralogical and chemical evidence: *Geol. Soc. Amer. Bull.* **87,** 725–737.

Huizinga, B. J., Tannenbaum, E., and Kaplan, I. R. (1987) The role of minerals in the thermal alteration of organic matter—IV. Generation of n-alkanes, acyclic isoprenoids, and alkenes in laboratory experiments: *Geochim. Cosmochim. Acta* **51,** 1083–1097.

Iijima, A. and Matsumoto, R. (1982) Berthierine and chamosite in coal measures of Japan: *Clays & Clay Minerals* **30,** 264–274.

Inoue, A. (1983) Potassium fixation by clay minerals during hydrothermal treatment. *Clays & Clay Minerals* **32,** 81–91.

Inoue, A. and Utada, M. (1983) Further investigations of a conversion series of dioctahedral mica/smectites in the Shinzan hydrothermal alteration area, northeast Japan. *Clays & Clay Minerals* **31,** 401–412.

McDowell, D. S. and Elders, W. A. (1980) Authigenic layer silicate minerals in borehole Elmore 1, Salton Sea geothermal field, California, U.S.A.: *Contr. Miner. Petrol.* **74,** 293–310.

Nadeau, P. H. and Reynolds, R. C. (1981) Burial and contact metamorphism in the Manco Shale: *Clays & Clay Minerals* **29,** 249–259.

Novich, K. and Martin, R. T. (1983) Solvation methods for expandable layers: *Clays & Clay Minerals* **31,** 235–238.

Pearson, M. J. and Small, J. S. (1988) Illite-smectite diagenesis and palaeotemperatures in northern North Sea Quaternary to Mesozoic shale sequences: *Clay Miner.* **23,** 109–132.

Ramseyer, K. and Boles, J. R. (1986) Mixed-layer illite/smectite minerals in Tertiary sandstones and shales, San Joaquin Basin, California: *Clays & Clay Minerals* **34,** 115–124.

Range, K. I., Range, A., and Weiss, A. (1969) Fire-type kaolinite or fire clay mineral? Experimental classification of kaolinite-halloysite minerals: in *Proc. Int. Clay Conf., Tokyo, Vol. I,* L. Heller, ed., Israel Univ. Press, Jerusalem, 3–13.

Reynolds, R. C. (1980) Interstratified clay minerals: in *Crystal Structures of Clay Minerals and their X-ray Identification,* G. W. Brindley and G. Brown, eds., Mineral. Soc., London, 249–303.

Reynolds, R. C. and Hower, J. (1970) The nature of interlayering in mixed layer illite-montmorillonite: *Clays & Clay Minerals* **18,** 25–36.

Roberson, H. E. and Lahann, R. W. (1981) Smectite to illite conversion rates: Effects of solution chemistry: *Clays & Clay Minerals* **29,** 129–135.

Rowsell, D. M. and De Swardt, A. M. J. (1976) Diagenesis in Cape and Karoo sediments, South Africa, and its bearing on their hydrocarbon potential: *Trans. Geol. Soc. S. Afr.* **79,** 81–145.

Saggerson, E. P. and Turner, L. M. (1988) Metamorphism in Phanerozoic rocks of southern Africa: *Extended abstracts, Geocongress '88,* University of Natal, Durban, 525–528.

Simoneit, B. R. T., Brenner, S., Peters, K. E., and Kaplan, I. R. (1981) Thermal alteration of Cretaceous black shale by diabase intrusions in the Eastern Atlantic—II. Effects on bitumen and kerogen: *Geochim. Cosmochim. Acta* **45,** 1581–1602.

Smart, G. and Clayton, T. (1985) The progressive illitization of interstratified illite-smectite from Carboniferous sediments of northern England and its relationship to organic maturity indicators: *Clay Miner.* **20,** 455–466.

Smith, D. A. M. and Whittaker, R. L. G. (1986) The coalfields of southern Africa: An introduction: in *Mineral Deposits of Southern Africa,* C. R. Anhaeusser and S. Maske, eds., *Geol. Soc. S. Afr.,* Johannesburg, 1875–1878.

South African Committee for Stratigraphy (SACS) (1980) Stratigraphy of South Africa, Pt.I: Lithostratigraphy of the Republic of South Africa, South West Africa/Namibia and the Republics of Bophutatswana, Transkei and Venda: *South Africa Geol. Surv. Handb.* **8,** 690 pp.

Środoń, J. (1979) Correlation between coal and clay diagenesis in the Carboniferous of the Upper Silesian Coal Basin: in *Proc. 6th Int. Clay Conf. Oxford, 1978,* M. M. Mortland and V. C. Farmer, eds., Elsevier, Amsterdam, 251–260.

Tissot, B. T., Pelet, R., and Ungerer, P. (1987) Thermal history of sedimentary basins, maturation indices, and kinetics of oil and gas generation: *Amer. Assoc. Petrol. Geol. Bull* **71,** 1445–1466.

Tomita, K., Takahashi, H., and Watanabe, T. (1988) Quantification curves for mica/smectite interstratifications by X-ray powder diffraction: *Clays & Clay Minerals* **36,** 258–262.

Van Vuuren, C. J. (1983) *A basin analysis of the northern facies of the Ecca Group:* Ph.D. thesis (unpubl.), Univ. Orange Free State, Bloemfontein, 249 pp.

Velde, B. (1985) *Clay minerals: A Physico-chemical Explanation of their Occurrence:* Elsevier, Amsterdam, 425 pp.

Whitney, G. (1990) Role of water in the smectite-to-illite reaction: *Clays & Clay Minerals* **38,** 343–350.

(Received 17 April 1991; accepted 25 November 1991; Ms. 2087)